Desalination and Water Treatment
www.deswater.com

doi: 10.1080/19443994.2013.839405

53 (2015) 530–542
January

Taylor & Francis
Taylor & Francis Group

Kinetics, equilibrium isotherms and thermodynamics of adsorption of Congo red onto natural and acid-treated kaolinite and montmorillonite

Krishna G. Bhattacharyya[a,*], Susmita Sen Gupta[b], Gautam Kumar Sarma[a]

[a]*Department of Chemistry, Gauhati University, Guwahati, Assam 781014, India*
Email: krishna2604@sify.com
[b]*Department of Chemistry, B N College, Dhubri, Assam 783324, India*

Received 25 June 2013; Accepted 24 August 2013

ABSTRACT

Naturally occurring kaolinite and montmorillonite were treated with 0.25 and 0.50 M H_2SO_4 and the modified clays along with the parent clays were used as adsorbents for the dye, Congo red in water. Adsorption was carried out in batch process with pH, dye concentration, amount of clay mineral, interaction time and temperature as the experimental variables. Adsorption was fast attaining equilibrium within 120 min and conforming to second-order kinetics. The Langmuir monolayer capacity for kaolinite and 0.25 M and 0.50 M acid-treated kaolinite varied from 0.024 to 0.033 mmol g^{-1}, 0.029 to 0.035 mmol g^{-1}, 0.030 to 0.036 mmol g^{-1}, respectively, in the temperature range of 293–323 K. The corresponding values for the montmorillonites were 0.223–0.243 mmol g^{-1}, 0.227–0.249 mmol g^{-1} and 0.231–0.256 mmol g^{-1}. Thermodynamic studies indicated that the dye molecules were held to the clay mineral surface by weak bonds and the whole process was endothermic near ambient temperature. The acid-treated clay minerals showed better adsorption capacity for the dye.

Keywords: Kaolinite; Montmorillonite; Acid treatment; Congo red; Adsorption; Isotherm

1. Introduction

Coloured effluents enter water from the production process of dyes and pigments and from industries using dyes or producing them as by-products, such as textile mills, pulp and paper industry, cosmetics manufacture, lather tanning, plastics, etc. Colour in natural water is not only aesthetically unacceptable, but it also interferes with the process of natural purification and disinfection of water by preventing sunlight penetration. It is also reported that colour in water might upset and interfere with the biological activities of the micro-organisms. Further, when the water is disinfected with chlorine-based chemicals such as bleaching powder, presence of dyes may lead to the formation of the toxic trihalomethanes [1,2].

Congo red [1-naphthalene sulphonic acid, 3,30-(4,40-biphenylenebis (azo))bis (4-amino-) disodium salt] is a benzidine-based anionic diazo dye, and is widely used in textile, paper, rubber and plastic industries [3]. Both, short time or prolonged contact of this dye with the eyes and skin causes severe irritation. On ingestion, it produces gastrointestinal irritation with nausea, vomiting and diarrhoea. It is

*Corresponding author.

known to be a carcinogenic, and prolonged use results in tumor formation amongst humans [4]. These human health concerns have led to discontinuation of the use of Congo red in many countries [5].

Removal of dyes and pigments from wastewater has been known to be a major challenge to the pollution control authorities. Most dyes are recalcitrant organic molecules, resistant to aerobic digestion and are stable to light, heat and oxidizing agents [6]. Adsorption onto a suitable solid has emerged as one of the most effective techniques for separation and removal of the dyes from water. Adsorption is both economical and feasible with the additional advantage of not producing toxic by-products with adverse impacts [7]. This has led to exploration of many novel and cheap materials as adsorbents for colour removal from water. A few of the recently tested materials include deoiled soya [7], hen feathers [8–11], bottom ash [12], wheat bran and rice bran [13], calcite [14], etc.

The clay minerals in soil play the role of a natural scavenger by filtering out pollutants from water through both ion exchange and adsorption mechanisms, and are considered as effective low-cost adsorbents for the removal of toxic dyes from water. Over the years, many clay minerals have been used for this purpose, e.g. kaolinite [15,16], natural and acid-activated bentonite [17], organo-vermiculite [18], thermal activated and acid-activated sepiolite [19], manganese oxide-coated sepiolite [20], etc. The high specific surface area, chemical and mechanical stability, layered structure, high cation exchange capacity (CEC), Brönsted and Lewis acidity, etc. have given excellent adsorption characteristics to the clay minerals [21]. Recent applications have tried to utilize either organo clays or pillared clays obtained by introducing large organic or inorganic groups into the interlayer space, but the use of these materials as adsorbents is often limited by the difficult modification process as well as the additional cost involved [17]. Instead, a simple and cost-effective modification by acid treatment has been found to produce better adsorbents by releasing octahedral Al atoms preferentially from the clay structure and leading to formation of additional Al–OH and Si–OH adsorption sites, without affecting the original mineral structure [22]. Acid treatment has also been shown to create higher porosity together with disaggregation and delamination of the clay platelets. While these changes serve to increase adsorption capacity, the use of stronger acid has the negative effect of decreasing adsorption capacity due to structural damage arising from partial dissolution of the clay mineral [23,24].

The present work was aimed at studying the adsorption capacity of kaolinite, montmorillonite and their acid-treated forms for adsorption of Congo red from aqueous solution under different experimental conditions.

2. Experimental set-up

2.1. Clays

Kaolinite, KGa-1b (K) and montmorillonite-K10 (M) were obtained from the University of Missouri, Columbia, Source Clay Minerals Repository, USA and Himedia Laboratory Private Limited, India, respectively. Acid-treated kaolinite (K1, 0.25 M H_2SO_4; K2, 0.50 M H_2SO_4) and montmorillonite (M1, 0.25 M H_2SO_4; M2, 0.50 M H_2SO_4) were prepared by the procedure of Espantaleon et al. [25]. About 20 g of clay was refluxed with 200 ml of either 0.25 M or 0.5 M H_2SO_4 for 3 h. The resulting material was centrifuged and washed with water several times till it was free of SO_4^{2-}, and then dried at 383 K in an air oven until constant weight. It is to be noted that only mild acid was used in the process to avoid structural damage to the clay minerals.

2.2. Characterization of clays

The adsorbents were characterized with XRD (Phillips Analytical PW 1710 Cu Kα radiations), SEM (Leo 1430VP), surface area and zeta potential (Malvern Zetasizer, Nanoseries ZS90) measurements. Surface area measurements were done with Sears' method [26] and the CEC was estimated by the procedure given by Bergaya and Vayer [27].

2.3. Preparation of Congo red solution

Congo red, $C_{32}H_{22}N_6Na_2O_6S_2$, (Loba Chemie, CI Classification Number: 22120; CAS No: 573-58-0; MW: 696.65) was used without further purification. The structure of the dye, Congo red is shown in Fig. 1.

A stock solution of the dye containing 1.435 mmol L^{-1} was first prepared by dissolving the required amount of dye in double distilled water. The aqueous solution of the dye had a pH of 6.94. Solutions for adsorption experiments were made from the stock solution in different concentrations.

2.4. Adsorption experiments

Before each experiment, blank runs were carried out by taking dye solutions in the same concentration

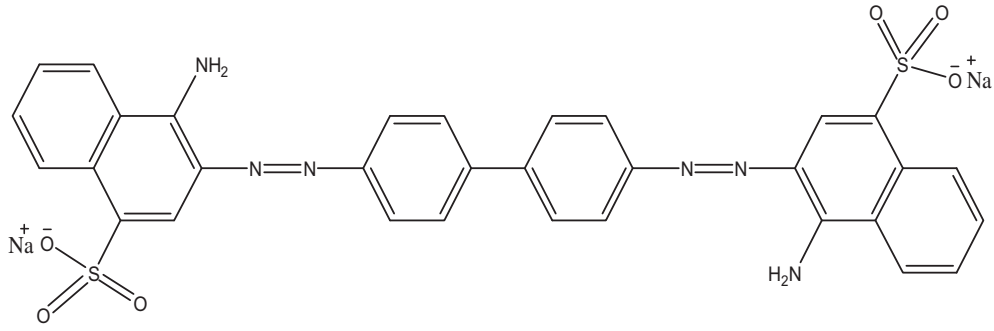

Fig. 1. Congo red structure.

range (as used in the adsorption experiments) in Erlenmeyer flasks without the clay adsorbents and shaking the same as in the actual experiments. The initial and final dye concentrations were almost constant showing that the walls of the flask did not show any measurable adsorption of the dye. The adsorption experiments were carried out in the same flasks by mixing a fixed amount of clay with 50 ml of aqueous dye solution. The mixture was agitated in a thermostatic water bath (NSW, Mumbai, India) for a pre-determined time interval. The mixture was centrifuged for 15 min (Remi R 24, ~10,000 rpm) and the remaining unadsorbed Congo red in the supernatant liquid was determined spectrophotometrically (Elico SL 177, India) at $\lambda = 499$ nm. All the experiments were done in triplicate to avoid experimental error. The standard deviation (SD) of the three sets of data was found to be very low (SD $\leqslant 0.0048$).

3. Results and discussion

3.1. Characterization of the clays and acid-activated clays

3.1.1. XRD measurement

Acid treatment and calcination are likely to influence the clay mineral structure, as H^+ ions replace some of the exchangeable cations on the surface. However, it was observed that there was only a little change in the intensity of the characteristic XRD peaks after acid treatment accompanied by slight broadening of the bands. The low-angle diffraction intensities showed some increase and there was a reduction in the corresponding tip widths. This is in agreement with other earlier XRD observations of the acid-treated clay minerals [28,29]. The following general comments could be made on the diffractograms (Fig. 2) of the acid-treated clay minerals:

(i) The basal spacing expanded from 7.14 to 7.16° Å ($2\theta = 12.34^\circ$) after treating kaolinite with 0.25 M H_2SO_4 (K1) and to 7.17° Å ($2\theta = 12.34^\circ$) after treating with 0.50 M H_2SO_4 (K2), accompanied by the decrease in intensity from 73.14 to 56.52% (K1) and 22.93% (K2).

(ii) The intensity of most of the low-angled XRD peaks of kaolinite showed some amount of positive change after acid treatment indicating enhancement of crystallinity of the clay minerals. The amorphous layer at the top might have been partially eroded by the acid such that both octahedral and tetrahedral sites could be reached directly by the X-ray beam.

(iii) The tip width of the $2\theta = 12.34^\circ$ peak in kaolinite reduced from 0.24 to 0.15 (K1) and 0.20 (K2). This is also an indication of the kaolinite surface becoming more visible to the X-ray beam after acid treatment such that the peaks became sharper.

Montmorillonite K-10 has a partially distorted structure which on treatment with a mineral acid at high temperature undergoes ion exchange, dealumination and extraction of iron and manganese [30]. In this work, however, acid treatment was carried out only under mild conditions using only dilute acid, and no drastic change in montmorillonite structure could be seen from the diffractograms. The montmorillonite K-10 showed peaks at 9.64 Å ($2\theta = 9.17^\circ$) and 18.06 Å ($2\theta = 4.91$) that suggested the presence of a clay mineral of mica group. Similar results were also obtained by Villegas et al. [31].

XRD of montmorillonite K-10 showed a layered structure with a basal spacing of 3.32 Å ($2\theta = 26.83^\circ$). After acid treatment, the basal spacing increased slightly to 3.35 Å (M1) and 3.34 Å (M2). Similar observations were reported for Cu-exchanged montmorillonite K-10 by Joseph et al. [32]. In the present work, the intensity of the peak at $2\theta = 18.05^\circ$ almost disappeared after acid treatment. Garade et al. [33] reported that impregnation of montmorillonite K-10 with 10

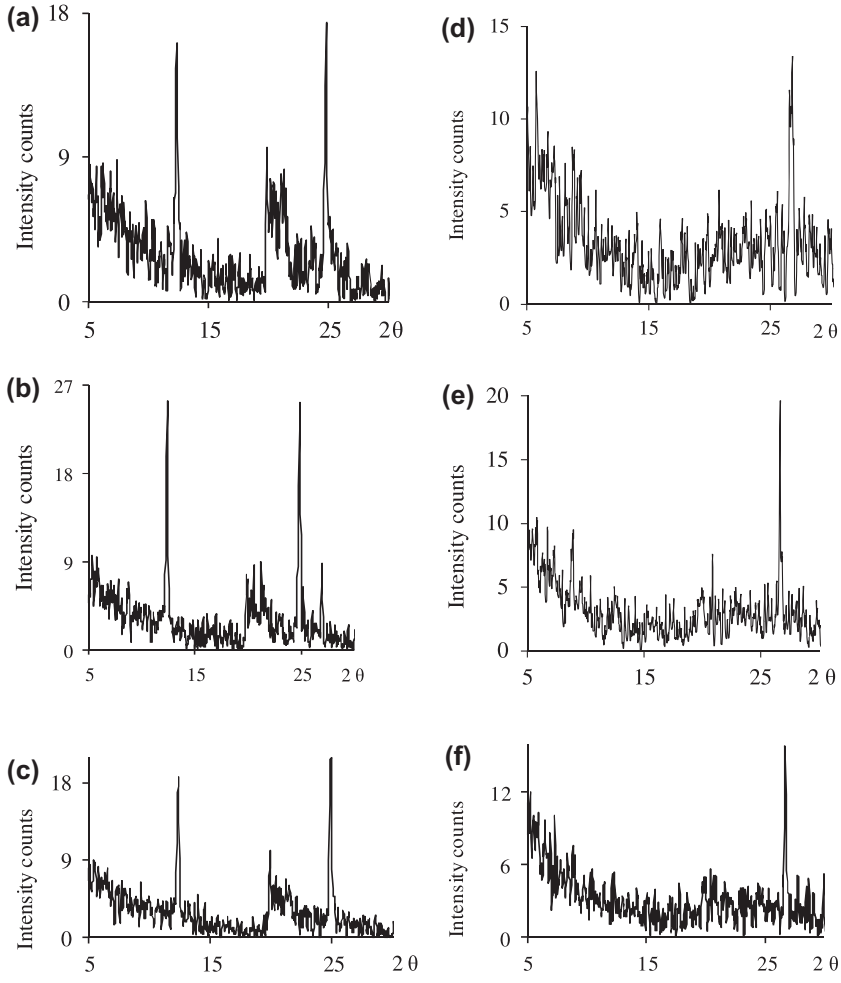

Fig. 2. XRD of (a) kaolinite K (b) 0.25 M acid-activated kaolinite K1 (c) 0.50 M acid-activated kaolinite K2 (d) montmorillonite M (e) 0.25 M acid-activated montmorillonite M1 (f) 0.50 M acid-activated montmorillonite M2.

and 20% dodecatungstophosphoric acid resulted in disappearance of the peak at $2\theta = 18^{\circ}$.

As a whole, the XRD measurements showed that the clay mineral structure remained intact even after acid treatment, and that the mild conditions of acid treatment had not distorted the clay mineral structure to any appreciable extent.

3.1.2. SEM measurement

SEM images of the six clay minerals are given in Fig. 3. The parent kaolinite showed solid hexagonal flakes as also found by other workers [34]. It also showed some white deposits on the surface of the flakes, which were likely to be non-clay minerals, e.g. oxides of sodium, potassium, calcium, iron and magnesium [35,36]. In case of montmorillonite, the flakes appeared smaller than those in kaolinite; the flakes had fluffy appearance indicating extremely fine platy structure. Similar micrographs had been reported by Molu and Yurdakoç [37]. White deposits over the flakes could be seen as in kaolinite. The surface morphology of both kaolinite and montmorillonite showed changes after acid treatment and the morphology appeared to have become more homogeneous. Similar observations were found in the literature [34]. Compared to 0.25 M acid, it was observed that 0.5 M acid did relatively more damage to the surface. It was also observed that acid treatment removed the deposits on the flakes and made the clay mineral surface clean.

3.1.3. Surface area measurement

The specific surface areas of kaolinite (K) and montmorillonite (M) were estimated as 3.8 and 92.6 m^2/g. The treatment with 0.25 M H_2SO_4 increased the surface area to 15.6 and 110.8 m^2/g for kaolinite

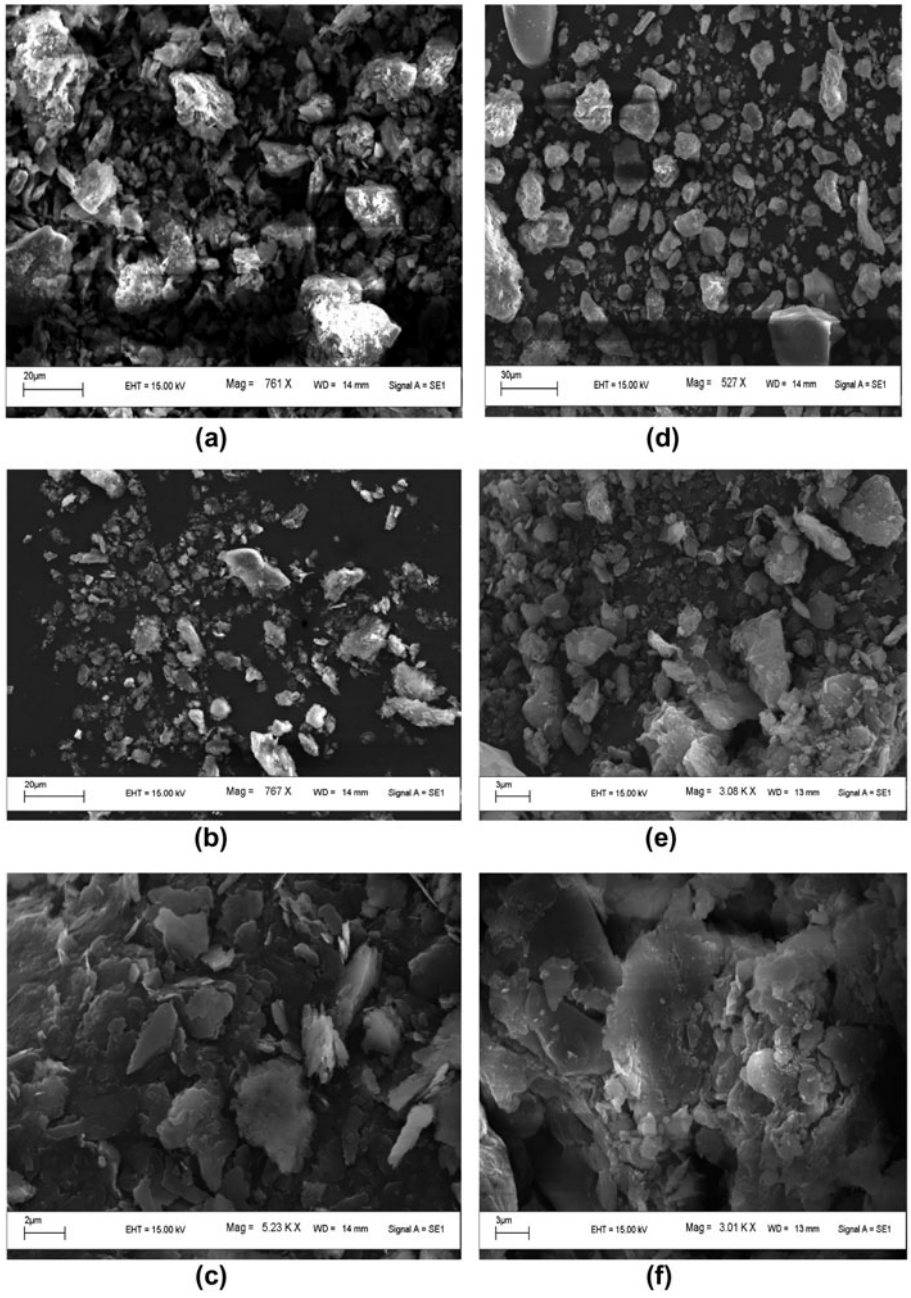

Fig. 3. SEM of (a) kaolinite K (b) 0.25 M acid-activated kaolinite K1 (c) 0.50 M acid-activated kaolinite K2 (d) montmorillonite M (e) 0.25 M acid-activated montmorillonite M1 (f) 0.50 M acid-activated montmorillonite M2.

(K1) and montmorillonite (M1), respectively. Further increase in acid strength (0.5 M H_2SO_4) enhanced the surface area to 19.2 (K2) and 131.2 (M2) m^2/g for kaolinite and montmorillonite, respectively. Similar changes were reported earlier [38,39]. The acid treatment opened up the edges of the platelets [29] and as a consequence the surface area and the pore diameter increased, which was in conformity with the results obtained in this work.

3.2. Congo red adsorption properties

3.2.1. Influence of pH

The pH is an important factor that often influences the mechanism of adsorption process. Congo red is a highly sensitive dye to pH. At pH <5.0, the dye changes its colour to blue, and at pH >10 a red colour is observed. This change in colour suggested that the dye had undergone structural changes [40].

The colour of Congo red is stable in the pH range of 6.0 to 10.0. Hence, the experiments were carried out in the pH range of 6.0 to 9.5 (Fig. 4).

The measurement of zeta potential showed that both kaolinite and montmorillonite did not have a zero point charge in the pH range used in the study (6.0–9.5). Kaolinite (K) had a zero point charge at pH 2.9 and therefore, kaolinite possessed a negative surface above this pH (2.9). On the other hand, raw montmorillonite did not show pH_{zpc} down to pH 2.0, a result consistent with the literature reports [41]. Substitution of Si with Al in the tetrahedral sheets and Al with Mg in the octahedral sheets of the 2:1 layer structure of montmorillonite had created a positive charge deficiency, which was responsible for the trend in zeta potential of the clay mineral. For acid-treated kaolinite, K1 and K2, pH_{zpc} shifted to pH 4 and pH 4.2, respectively and showed a general decrease in negative charge in the clay surface. Acid-treated montmorillonite M1 and M2 also showed an increase in positive charge on the surface and showed pH_{zpc} at pH 2 and pH 3.6, respectively. This might be due to the increased acidity of the clay surface. Ma et al. [42] also reported an increase in pH_{zpc} of bentonite after modification.

It was observed that for all the six clay minerals, low pH favored adsorption of the dye. As is shown above from zeta potential measurements, the clay mineral surface became more negative at higher pH and the Congo red anions would therefore prefer a less negative surface (low pH) to bind to the adsorbent surface. The dye anions might also be held through specific adsorption. There might also be a competition between OH^- (at high pH) and Congo red anions for specific adsorption on the negatively charged clay mineral surface, and highly mobile OH^- ions were likely to be preferentially adsorbed in comparison to the bulky dye anions. Still, significant adsorption was observed in the pH range of 7.0 to 9.5, suggesting chemisorption to be operative in this pH range [40].

3.2.2. Kinetics of adsorption

The clay minerals took up the dye anions at a very fast rate (Fig. 5) for the first 30 min and equilibrium was attained within 120 min. Montmorillonite showed significantly higher adsorption capacity than kaolinite and its acid-treated forms. With initial dye concentration of 0.144 mmol L^{-1}, kaolinite (2.0 g L^{-1}) removed ~16% of the dye within the first 5 min and ~27% in 120 min (pH 6.9, temperature 303 K). In case of montmorillonite (0.4 g L^{-1}), 14% of the dye (0.144 mmol L^{-1}) was removed within 5 min and ~22% after 120 min, close to equilibrium, under similar experimental conditions. The rate processes suggested that the clay minerals interacted with the dye in two stages: a rapid removal stage followed by a much slower stage before the equilibrium was established. At the initial stage, large numbers of active sites on the clay minerals were available for dye anions and the rate of adsorption was high. As the fraction of the bare surface rapidly diminished, the adsorption rate came down and thus, dye anions were competing among themselves for the adsorption sites. The rate was then predominantly influenced by the rate at which Congo red molecules were transported from the bulk to the adsorbate/adsorbent interface.

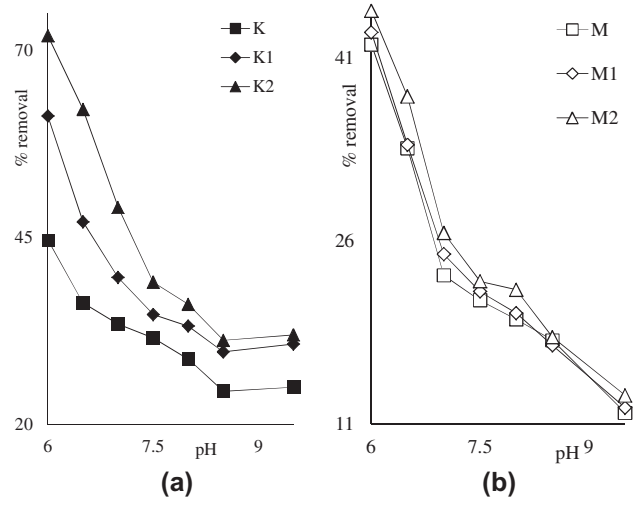

Fig. 4. Influence of pH for Congo red adsorption on (a) kaolinites and (b) montmorillonites at 303 K.

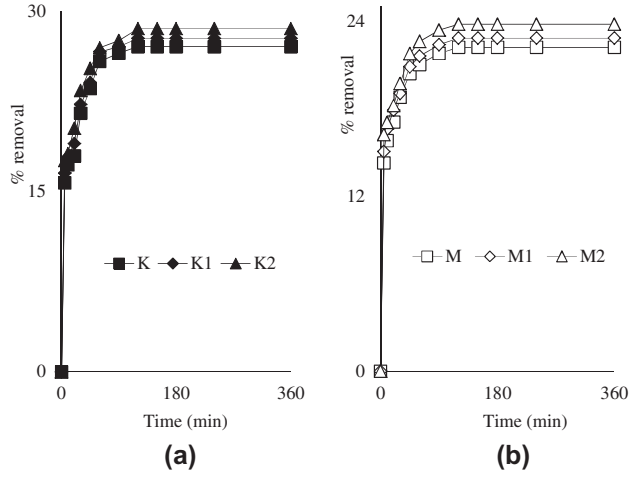

Fig. 5. Influence of interaction time for Congo red adsorption on (a) kaolinites and (b) montmorillonites at 303 K.

The kinetics of the interactions were thus likely to be dependent on different rate processes as the interaction time increased [3].

Different kinetic models were used to find out how the clays were interacting with the dye molecules. The first-order Lagergren model was tested by plotting ln (q_e–q_t) vs. time according to the equation [43],

$$\text{In } (q_e - q_t) = \text{In } q_e - k_1 t \quad (1)$$

where q_e and q_t are the amounts adsorbed per unit mass at equilibrium and at any time t, and k_1 is the first-order rate coefficient. The values of k_1 obtained from the plots ($r \sim$ –0.99) varied from 3.06×10^{-2} to 3.78×10^{-2} min^{-1} at 303 K for the six adsorbents (Table 1) indicating first-order to be the likely mechanism. However, inconsistency arose when the equilibrium solid–liquid phase concentrations of the dye, q_e obtained from the plots were compared with the experimental q_e values, the deviations being too large (–145.21 to +99.75%, Table 1). Lagergren type of kinetics was therefore rejected and the validity of second-order kinetics was tested.

The second-order plots [44] of t/q_t vs. t from the linear relation,

$$t/q_t = 1/(k_2 q_e^2) + (1/q_e)t \quad (2)$$

yielded better linearity ($r \sim$ +0.99, Fig. 6) and the second-order rate coefficient at 303 K varied from 1.98 to 5.33 g $mmol^{-1}$ min^{-1} for the six adsorbents (Table 2). The experimental q_e values now showed much better agreement with those obtained from the plots (Table 2) with deviations limited to +2.03 to +4.88%. It is thus concluded that the clays took up the dye anions through a second-order mechanism and the rate determining step involved two anions of the dye.

Since the clay mineral surface is expected to be energetically heterogeneous, the Elovich equation [45],

$$q_t = \beta \ln (\alpha\beta) + \beta \ln t \quad (3)$$

applicable for such sorbents was also tested. The Elovich coefficients, α and β (Table 3), represent the initial adsorption rate (g mol^{-1} min^2) and the desorption coefficient (mol g^{-1} min^{-1}), respectively. In conformity with Eq. (3), the plots of q_t vs. ln t had good linearity and thus, the dye anions were likely to bind to sites on the clay surface in order of increasing energy.

3.2.3. Influence of clay amount

For initial dye concentration of 0.144 mmol L^{-1}, the clay minerals (1–6 g L^{-1} for kaolinites and 0.2–0.6 g L^{-1} for montmorillonites; pH 6.9, temperature 303 K) adsorbed different amounts of the dye: 17.34–56.41% by kaolinite (K), 18.55–57.3% by 0.25 M acid-treated kaolinite (K1), 19.23–58.32% by 0.5 M acid-treated kaolinite (K2), 16.12–29.02% by montmorillonite (M), 16.71–30.01% by 0.25 M acid-treated montmorillonite (M1) and 17.27–31.81% by 0.5 M acid-treated montmorillonite (M2). The increased adsorption with the increase in clay mineral amount was obvious as an increase in adsorbent amount made available a larger number of adsorption sites for the dye anions.

Despite the increase in the extent of adsorption, the amount of dye adsorbed per unit mass of clay showed (q_e) a decrease with an increase in clay amount (K: 0.024–0.013 mmol g^{-1}, K1: 0.027–0.014 mmol g^{-1}, K2: 0.028–0.015 mmol g^{-1}, M: 0.116–0.069 mmol g^{-1}, M1:0.120–0.072 mmol g^{-1}, M2: 0.124–0.076 mmol g^{-1}). It was likely that the increase in clay mineral amount resulted in particle aggregation and consequently a decrease in the surface area and an increase in diffusional path length [46].

Table 1
Lagergren first-order rate coefficients and q_e values for Congo red adsorption on clay minerals (kaolinites 2.0 g L^{-1}, montmorillonites 0.4 g L^{-1}, dye concentration 0.144 mmol L^{-1}, pH 6.94)

Clay mineral	Lagergren coefficient		q_e (mmol g^{-1})		
	$k_1 \times 10^2$ (min^{-1})	r	Experimental	Lagergren	Deviation (%)
K	3.78	−0.99	0.0195	7.9080	+99.75
K1	3.59	−0.98	0.0199	7.4740	+99.73
K2	3.06	−0.99	0.0205	6.6720	+99.63
M	3.50	−0.99	0.0796	0.0340	−134.12
M1	3.36	−0.99	0.0819	0.0334	−145.21
M2	3.54	−0.99	0.0853	0.0364	−134.34

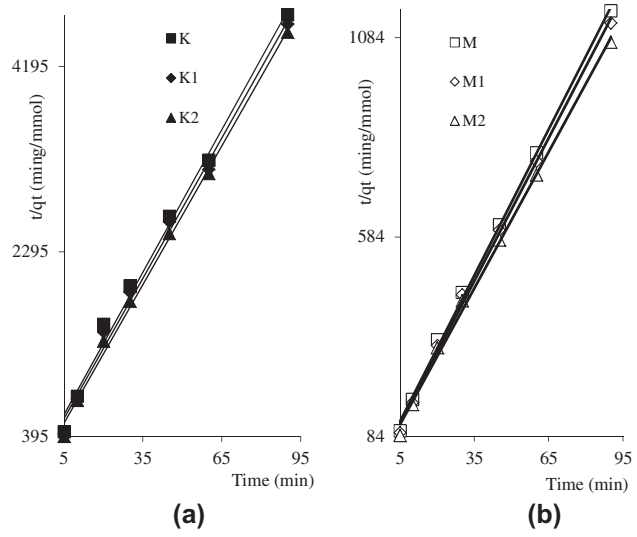

Fig. 6. Second-order plots for Congo red adsorption on (a) kaolinites and (b) montmorillonites at 303 K.

3.2.4. Influence of initial dye concentration

The uptake of dye by the clay minerals decreased when the Congo red concentration was increased. However, the amount adsorbed per unit mass, q_e, showed an increasing trend; q_e increased from 0.013 to 0.025 mmol g^{-1}, 0.014 to 0.028 mmol g^{-1}, 0.015 to 0.030 mmol g^{-1} for K, K1 and K2, respectively, (dye 0.072 to 0.502 mmol L^{-1}) and 0.065 to 0.0158 mmol g^{-1} (M), 0.067 to 0.164 mmol g^{-1} (M1) and 0.068 to 0.168 mmol g^{-1} (M2) (dye 0.115 to 0.574 mmol L^{-1}).

At low initial dye concentration, the ratio of the number of Congo red anions to the number of available adsorption sites was small and consequently the adsorption was independent of the initial concentration. The dye cations were driven to the clay mineral surface by the force generated due to the concentration gradient between the clay mineral surface and the bulk solution. Under the same conditions, if the concentration of the dye was high, the active sites on the clay mineral would be surrounded by many more dye molecules, and the active sites were likely to take up their full quota of dye molecules depending on the degree of unsaturation. Thus, q_e values increased with the increase in initial dye concentration.

3.2.5. Adsorption isotherm

The adsorption capacity and the affinity of a particular adsorbent towards a particular adsorbate are best obtained from the isotherms. Two of the isotherms receiving maximum attention are the linear versions of Freundlich [47] (Eq. (4)) and Langmuir [48] (Eq. (5)) isotherms:

$$\log q_e = n \log C_e + \log K_f \quad (4)$$

Table 2
Second-order rate coefficients and q_e values for Congo red adsorption on clay minerals (kaolinites 2.0 g L^{-1}, montmorillonites 0.4 g L^{-1}, dye concentration 0.144 mmol L^{-1}, pH 6.94)

Clay mineral	Second-order coefficient		q_e (mmol g^{-1})		
	k_2 (g mmol^{-1} min^{-1})	r	Experimental	Second-order	Deviation (%)
K	5.33	+0.99	0.0195	0.0205	+4.88
K1	4.61	+0.99	0.0199	0.0209	+4.78
K2	5.12	+0.99	0.0205	0.0211	+2.84
M	1.98	+0.99	0.0796	0.0818	+2.69
M1	2.17	+0.99	0.0819	0.0836	+2.03
M2	2.21	+0.99	0.0853	0.0877	+2.74

Table 3
Elovich coefficients for Congo red adsorption on clay minerals (kaolinites 2.0 g L^{-1}, montmorillonites 0.4 g L^{-1}, dye concentration 0.144 mmol L^{-1}, pH 6.94)

Clay mineral	K	K1	K2	M	M1	M2
α (g mol^{-1} min^{2})	1.83×10^3	3.91×10^3	1.0×10^4	4.72	8.17	9.55
β (mol g^{-1} min^{-1})	0.82	0.80	0.78	6.86	6.86	6.70
r	+0.97	+0.97	+0.97	+0.99	+0.99	+0.97

$$C_e/q_e = 1/(bq_m) + (1/q_m)C_e \quad (5)$$

where C_e is the equilibrium concentration of the dye (mmol L^{-1}); q_e is the amount of the dye adsorbed per mass unit of adsorbent (mmol g^{-1}). K_f (mmol$^{1-1/n}$ $L^{1/n}$ g^{-1}) and n, the Freundlich coefficients, represent adsorption capacity and adsorption intensity, respectively, and can be estimated from the intercept and slope of the linear plots of log q_e vs. log C_e. For favourable adsorption, n is <1. The Langmuir coefficients, q_m (amount adsorbed to form a monolayer over the clay mineral surface, mmol g^{-1}) and b (the equilibrium constant of clay mineral–dye interactions, L $mmol^{-1}$) were obtained from the plots of C_e/q_e vs. C_e.

The Freundlich isotherms at 303 K were linear (r$\sim$ + 0.94 to + 0.99, Fig. 7) with the adsorption coefficients n (0.29–0.50) and K_f 0.034–0.041 mmol$^{1-1/n}$L$^{1/n}$ g^{-1} for kaolinite and its acid-treated forms, and 0.226 to 0.240 mmol$^{1-1/n}$L$^{1/n}$ g^{-1} for montmorillonite and its acid-treated forms (Table 4). Similar trends were found at other temperatures as well. The adsorption capacities (K_f) were in the order of M2 > M1 > M > K2 > K1 > K. The Langmuir plots too were linear (r $\sim$ + 0.99, Fig. 8) and the equilibrium coefficient, b (Table 5), was large enough for a favourable shift of the equilibrium towards the formation of dye-clay sorption complex.

By changing the adsorption temperature from 293 to 323 K, q_m increased from 0.024 to 0.033 mmol g^{-1}, 0.029 to 0.035 mmol g^{-1}, 0.030 to 0.036 mmol g^{-1}, 0.223 to 0.243 mmol g^{-1}, 0.227 to 0.249 mmol g^{-1} and 0.231 to 0.256 mmol g^{-1} for K, K1, K2, M, M1 and M2, respectively (Table 5). q_m had a similar order as the Freundlich adsorption capacity, i.e. M2 > M1 > M > K2 > K1 > K. Acid activation had resulted in an increase in the Langmuir monolayer capacity, q_m, for both kaolinite and montmorillonite. Acid treatment enhanced the Langmuir capacity of kaolinite by $\sim$10.71% for K1 (from 0.028 to 0.031 mmol g^{-1}) and $\sim$17.86% for K2 (from 0.028 to 0.033 mmol g^{-1}), but montmorillonite had only small enhancement (from 0.227 to 0.232 mmol g^{-1}, 2.20% for M1 and 0.227 to 0.236 mmol g^{-1}, 3.96% for M2) at 303 K. Acid treatment, thus, generated a considerable number of additional adsorption sites in case of kaolinite, but this influence was not much in the case of montmorillonite. The acid treatments were known to eliminate

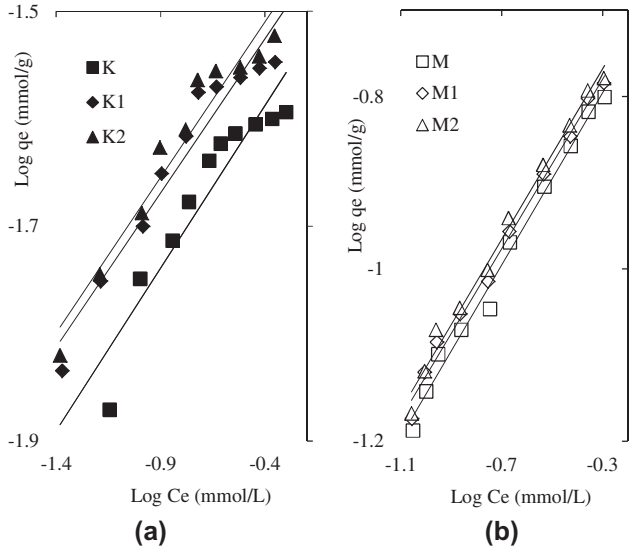

Fig. 7. Freundlich plots for adsorption of Congo red on (a) kaolinites and (b) montmorillonites.

Table 4
Freundlich coefficients for Congo red adsorption on clay minerals (kaolinites 2.0 g L^{-1}, montmorillonites 0.4 g L^{-1}, initial dye concentration 0.072–0.502 mmol L^{-1} for kaolinites and 0.115–0.574 mmol L^{-1} for montmorillonites, pH 6.94)

Temp (K)	Freundlich coefficient	Clay minerals					
		K	K1	K2	M	M1	M2
293	k_f (mmol$^{1-1/n}$ $L^{1/n}$ g^{-1})	0.028	0.035	0.036	0.233	0.239	0.244
	n	0.27	0.32	0.32	0.54	0.53	0.51
	r	+0.98	+0.97	+0.97	+0.98	+0.98	+0.98
303	k_f (mmol$^{1-1/n}$ $L^{1/n}$ g^{-1})	0.034	0.039	0.041	0.226	0.233	0.240
	n	0.30	0.29	0.29	0.50	0.49	0.50
	r	+0.94	+0.97	+0.97	+0.99	+0.99	+0.99
313	k_f (mmol$^{1-1/n}$ $L^{1/n}$ g^{-1})	0.035	0.041	0.055	0.242	0.253	0.261
	n	0.22	0.26	0.26	0.46	0.47	0.47
	r	+0.98	+0.96	+0.96	+0.99	+0.99	+0.99
323	k_f (mmol$^{1-1/n}$ $L^{1/n}$ g^{-1})	0.039	0.042	0.043	0.263	0.267	0.276
	n	0.24	0.25	0.24	0.41	0.40	0.40
	r	+0.99	+0.99	+0.97	+0.99	+0.98	+0.99

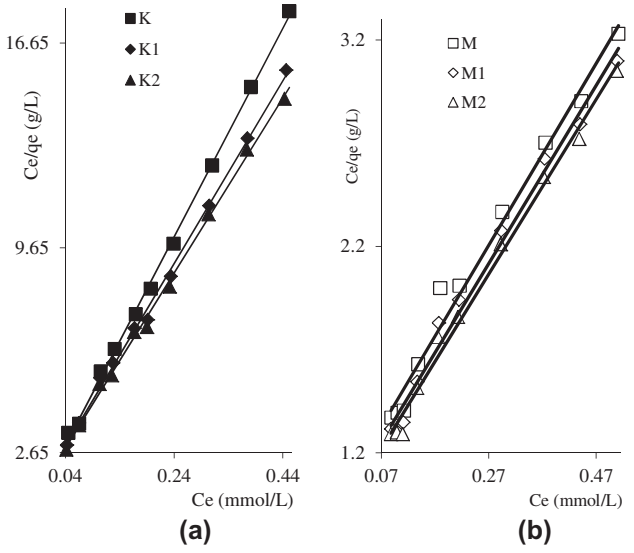

Fig. 8. Langmuir plots for Congo red adsorption on (a) kaolinites and (b) montmorillonites at 303 K.

mineral impurities from the surface [49] with partial dissolution of the external layers. This might also be a contributing factor in the less-than-expected increase in adsorption capacity after acid treatment. Similar results were also reported earlier [50].

The monolayer adsorption capacity (q_m) of Congo red on bentonite [40] was 0.228 mmol g^{-1}. Vimonses et al. [34] have found that locally available kaolinite samples have monolayer capacity of 0.008–0.014 mmol g^{-1} for Congo red. γ-Fe_2O_3 has a much larger monolayer capacity of 0.299 mmol g^{-1} at pH 5.9 [5].

3.2.6. Thermodynamics of Congo red adsorption on clays

The amount of dye adsorbed per unit mass of clay mineral (q_m) increased when the adsorption temperature raised from 293 to 323 K, indicating endothermic interactions. Adsorption of Congo red on clay minerals, thus, required small activation energy and the rise in temperature facilitated more dye anions to overcome the energy barrier and get attached to the surface. Similar endothermic interactions of Congo red had been reported earlier [51].

The thermodynamic adsorption parameters, ΔH, ΔS and ΔG (Table 6), were computed from the plots of ln K_d vs. $1/T$ from the equations,

$$\ln K_d = (\Delta S/R) - (\Delta H/RT) \quad (6)$$

$$\Delta G = \Delta H - T\Delta S \quad (7)$$

where K_d (q_e/C_e) is known as the distribution coefficient, T the temperature (K) and $R = 8.314 \times 10^{-3}$ kJ K^{-1} mol^{-1}. The mean adsorption enthalpy, ΔH, varied from 10.21 to 11.75 kJ mol^{-1} for the kaolinites and from 9.73 to 9.93 kJ mol^{-1} for montmorillonites. The clay surface thus holds the dye anions with weak interactive forces.

Entropy of adsorption, ΔS, had increased for all the clay minerals in the temperature range of 293 to 323 K and the mean ΔS varied from 17 to 27 J K^{-1} mol^{-1} for the six adsorbents. Since the interactions did not bring about any major change in surface configuration, the entropy increase that could be

Table 5
Langmuir coefficients for Congo red adsorption on clay minerals (kaolinites 2.0 g L^{-1}, montmorillonites 0.4 g L^{-1}, initial dye concentration 0.072–0.502 mmol L^{-1} for kaolinites and 0.115–0.574 mmol L^{-1} for montmorillonites, pH 6.94)

Temp (K)	Langmuir coefficient	Clay minerals					
		K	K1	K2	M	M1	M2
293	q_m (mmol g^{-1})	0.024	0.029	0.030	0.223	0.227	0.231
	b (L $mmol^{-1}$)	18.45	14.98	15.09	4.26	4.40	4.79
	r	+0.99	+0.99	+0.99	+0.99	+0.99	+0.99
303	q_m (mmol g^{-1})	0.028	0.031	0.033	0.227	0.232	0.236
	b (L $mmol^{-1}$)	24.23	19.36	18.52	4.33	4.54	4.60
	r	+0.99	+0.99	+0.99	+0.99	+0.99	+0.99
313	q_m (mmol g^{-1})	0.030	0.034	0.035	0.235	0.244	0.251
	b (L $mmol^{-1}$)	23.76	20.92	22.87	5.24	5.20	5.21
	r	+0.99	+0.99	+0.99	+0.99	+0.99	+0.99
323	q_m (mmol g^{-1})	0.033	0.035	0.036	0.243	0.249	0.256
	b (L $mmol^{-1}$)	21.95	22.85	24.15	7.09	7.32	7.45
	r	+0.99	+0.99	+0.99	+0.99	+0.99	+0.99

Table 6
Thermodynamic data for Congo red adsorption on clay minerals (kaolinites 2 g L^{-1}, montmorillonites 0.4 g L^{-1}, initial dye concentration 0.072–0.502 mmol L^{-1} for kaolinites and 0.115–0.574 mmol L^{-1} for montmorillonites, pH 6.94)

Clay minerals	ΔH (kJ mol^{-1})	ΔS (J K^{-1} mol^{-1})	ΔG (kJ mol^{-1})			
			293 K	303 K	313 K	323 K
K	11.75	21	5.64	5.43	5.22	5.01
K1	10.67	19	5.20	5.02	4.83	4.64
K2	10.21	17	5.12	4.95	4.95	4.60
M	9.80	27	1.92	1.65	1.38	1.11
M1	9.73	27	1.84	1.57	1.30	1.04
M2	9.93	26	2.42	2.16	1.91	1.65

attributed to random distribution of the dye molecules on the clay surface was not much. The structural adjustments in the dye molecules as they were held through weak forces [52] might also have contributed to the entropy increase. The dye anions interacted with H^+ and K^+ ions on the clay mineral surface and brought about adsorption of the dye [53]. The small entropy increase could drive the endothermic interactions. Gibbs energy for the process, ΔG, decreased from 5.64 to 5.01 kJ mol^{-1} (K), 5.20 to 4.64 kJ mol^{-1} (K1), 5.12 to 4.60 kJ mol^{-1} (K2), 1.92 to 1.11 kJ mol^{-1} (M), 1.84 to 1.04 kJ mol^{-1} (M1) and 2.42 to 1.65 kJ mol^{-1} (M2) in the temperature range of 293 to 323 K, which agreed with the endothermic nature of the interactions. Tomul [54] had reported similar positive ΔG results for the adsorption of Cd^{2+} on Fe/Cr pillared bentonite. Auta and Haeed [55] also reported positive ΔG values for methelyne blue adsorption by raw ball clay.

3.3. Adsorption mechanism

In the light of the kinetics and isotherm studies, it is observed that the adsorption followed second-order kinetics. Since montmorillonite swells in contact with water giving more space for Congo red anions to enter into the cavity, this clay mineral had higher sorption capacity. At natural pH (6.94), Congo red is present in aqueous state in non-protonated form [56] and thus, adsorption may not occur through proton exchange. Since quite a large amount of the dye was taken up by the clay minerals, which had low anion exchange capacity (anion exchange capacity of montmorillonite is less than that of kaolinite), anion exchange as a mechanism of adsorption may also be ruled out [57]. Therefore, two other possibilities have to be considered: either adsorption occurred through an acid–base type of interaction with the clay mineral providing an acidic surface and Congo red anions were taken up as the basic entity [40], or there might be a complexation reaction through the two primary amine ($-NH_2$) groups attached to the naphthalene rings in the Congo red molecule [58]. Specific adsorption was also not ruled out.

4. Conclusion

Kaolinite, montmorillonite and the acid-treated forms are capable of removing Congo red from aqueous solution. Acid treatment enhances the adsorption capacity compared to the untreated clay minerals due to the increased surface area.

The clay mineral–dye interactions were very fast in the first 30 min and attained equilibrium within 120 min. The dye anions were held following second-order kinetics and the clay minerals had monolayer capacity of 0.028 (kaolinite) to 0.236 mmol g^{-1} (acid-treated montmorillonite) at 303 K. These values showed that the clay minerals could hold quite a significant amount of the dye on the surface leading to its separation from an aqueous solution. In the temperature range around ambient temperature, the Congo red adsorption was endothermic, accompanied by an increase in entropy and a decrease in Gibbs energy.

Acknowledgement

The authors are grateful to the University Grants Commission, New Delhi for providing assistance under a Major Research Project for this work. The authors acknowledge the use of the SEM facility at CIF, IIT Guwahati, and XRD at SIF, Gauhati University. The authors also thank Upama Baruah of IASST, Guwahati, for her help in taking zeta potential measurements.

References

[1] J. Anandkumar, B. Mandal, Adsorption of chromium (VI) and rhodamine B by surface modified tannery waste: Kinetic, mechanistic and thermodynamic studies, J. Hazard. Mater. 186 (2011) 1088–1096.

[2] A.E. Vasu, Studies on the removal of rhodamine B and malachite green from aqueous solutions by activated carbon, e-J. Chem. 5 (2008) 844–852. http://www.e-journals.net.
[3] Z. Hu, H. Chena, F. Ji, S. Yuana, Removal of Congo red from aqueous solution by cattail root, J. Hazard. Mater. 173 (2010) 292–297.
[4] A. Mittal, V. Thakur, J. Mittal, H. Vardhan, Process development for the removal of hazardous anionic azo dye Congo red from wastewater by using hen feather as potential adsorbent, Desalin. Water Treat. doi: 10.1080/19443994.2013.785030.
[5] A. Afkhami, R. Moosavi, Adsorptive removal of Congo red, a carcinogenic textile dye, from aqueous solutions by maghemite nanoparticles, J. Hazard. Mater. 174 (2010) 398–403.
[6] G. Crini, Non-conventional low-cost adsorbents for dye removal: A review, Bioresour. Technol. 97 (2006) 1061–1085.
[7] A. Mittal, D. Jhare, J. Mittal, Adsorption of hazardous dye Eosin Yellow from aqueous solution onto waste material De-oiled Soya: Isotherm, kinetics and bulk removal, J. Mol. Liq. 179 (2013) 133–140.
[8] A. Mittal, V. Thakur, V. Gajbe, Evaluation of adsorption characteristics of an anionic azo dye Brilliant Yellow onto hen feathers in aqueous solutions, Environ. Sci. Pollut. Res. 19 (2012) 2438–2447.
[9] A. Mittal, V. Thakur, V. Gajbe, Adsorptive removal of toxic azo dye Amido Black 10B by hen feather, Environ. Sci. Pollut. Res. 20 (2013) 260–269.
[10] A. Mittal, L. Kurup, J. Mittal, Freundlich and Langmuir adsorption isotherms and kinetics for the removal of Tartrazine from aqueous solutions using hen feathers, J. Hazard. Mater. 146 (2007) 243–248.
[11] A. Mittal, J. Mittal, L. Kurup, Utilization of hen feathers for the adsorption of Indigo Carmine from simulated effluents, J. Environ. Prot. Sci. 1 (2007) 92–100.
[12] V.K. Gupta, A. Mittal, D. Jhare, J. Mittal, Batch and bulk removal of hazardous colouring agent Rose Bengal by adsorption techniques using bottom ash as adsorbent, RSC Adv. 2 (2012) 8381–8389.
[13] X.S. Wang, J.P. Chen, Biosorption of Congo red from aqueous solution using wheat bran and rice bran: Batch studies, Sep. Sci. Technol. 44 (2009) 1452–1466.
[14] G. Atun, E.T. Acar, Competitive adsorption of basic dyes onto calcite in single and binary component systems, Sep. Sci. Technol. 45 (2010) 1471–1481.
[15] D. Ghosh, K.G. Bhattacharyya, Adsorption of methylene blue on kaolinite, Appl. Clay Sci. 20 (2002) 295–300.
[16] B.K. Nandi, A. Goswami, M.K. Purkait, Adsorption characteristics of brilliant green dye on kaolin, J. Hazard. Mater. 161 (2009) 387–395.
[17] B. Benguella, A. Yacouta-Nour, Adsorption of bezanyl red and nylomine green from aqueous solutions by natural and acid-activated bentonite, Desalination 235 (2009) 276–292.
[18] X. Yu, C. Wei, L. Ke, Y. Hu, X. Xie, H. Wu, Development of organovermiculite-based adsorbent for removing anionic dye from aqueous solution, J. Hazard. Mater. 180 (2010) 499–507.
[19] M. Uğurlu, Adsorption of a textile dye onto activated sepiolite, Microporous Mesoporous Mater. 119 (2009) 276–283.
[20] E. Eren, O. Cubuk, H. Ciftci, B. Eren, B. Caglar, Adsorption of basic dye from aqueous solutions by modified sepiolite: Equilibrium, kinetics and thermodynamics study, Desalination 252 (2010) 88–96.
[21] K. Tanabe, Solid acid and base catalysis, In: J.R. Anderson, M. Boudart (Eds), Catalysis Science and Technology, Springer-Verlag, Berlin, pp. 231–273, 1981.
[22] G. Suraj, C.S.P. Iyer, M. Lalithambika, Adsorption of cadmium and copper by modified kaolinite, Appl. Clay Sci. 13 (1998) 293–306.
[23] B. Tyagi, C.D. Chudasama, R.V. Jasra, Determination of structural modification in acid activated montmorillonite clay by FT–IR spectroscopy, Spectrochimica Acta, Part A 64 (2006) 273–278.
[24] Y.E. Mouzdahir, A. Elmchaouri, R. Mahboub, A. Gil, S.A. Korili, Equilibrium modeling for the adsorption of methylene blue from aqueous solutions on activated clay minerals, Desalination 250 (2010) 335–338.
[25] A.G. Espantaleon, J.A. Nieto, M. Fernandez, A. Marsal, Use of activated clays in the removal of dyes and surfactants from tannery waste waters, Appl. Clay Sci. 24 (2003) 105–110.
[26] G.W. Sears, Determination of specific surface area of colloidal silica by titration with sodium hydroxide, Anal. Chem. 28 (1956) 1981–1983.
[27] F. Bergaya, M. Vayer, CEC of clays: Measurement by adsorption of a copper ethylendiamine complex, Appl. Clay Sci. 12 (1997) 275–280.
[28] G. Jozefaciuk, G. Bowanko, Effect of acid and alkali treatments on surface areas and adsorption energies of selected minerals, Clays Clay Miner. 50 (2002) 771–783.
[29] F.R.V. Diaz, P.S. Santos, Studies on the acid activation of Brazilian smectitic clay, Quim. Nova 24 (2001) 345–353.
[30] T. Cseri, S. Békássy, F. Figueras, E. Cseke, L.C. de Menorval, R. Dutartre, Characterization of clay-based K catalyst and their application in Friedel-Crafts alkylation of aromatics, Appl. Catal. A 132 (1995) 141–155.
[31] R.A.S. Villegas, J.L.D.E. Santo, Jr, M.C.S. de Mattos, M.R.M.P. de Aguiar, A.W.S. Guarino, Characterization of natural Brazilian clays and their utilization as catalysts in the coiodination of alkenes with water and alcohols, J. Braz. Chem. Soc. 16 (2005) 565–570.
[32] T. Joseph, G.V. Shanbhag, S.B. Halligudi, Copper (II) ion-exchanged montmorillonite as catalyst for the direct addition of N–H bond to C–C triple bond, J. Mol. Catal. A: Chem. 236 (2005) 139–144.
[33] A.C. Garade, V.S. Kshirsagar, R.B. Mane, A.A. Ghalwadkar, U. D. Joshi, C.V. Rode, Acidity tuning of montmorillonite K10 by impregnation with dodecatungstophosphoric acid and hydroxyalkylation of phenol, Appl. Clay Sci. 48 (2010) 164–170.
[34] V. Vimonses, S. Lei, B. Jin, C.W.K. Chow, C. Saint, Adsorption of Congo red by three Australian kaolins, Appl. Clay Sci. 43 (2009) 465–472.
[35] E. Galan, P. Aparicio, A. Miras, K. Michailidis, A. Tsirambides, Technical properties of compounded kaolin sample from Griva (Macedonia, Greece), Appl. Clay Sci. 10 (1996) 477–490.
[36] E.I. Unuabonah, K.O. Adebowale, B.I. Olu-Owolabi, L.Z. Yang, Comparison of sorption of Pb^{2+} and Cd^{2+} on kaolinite clay and polyvinyl alcohol-modified kaolinite clay, Adsorption 14 (2008) 791–803.
[37] Z.B. Molu, K. Yurdakoc, Preparation and characterization of aluminum pillared K10 and KSF for adsorption of trimethoprim, Microporous Mesoporous Mater. 127 (2010) 50–60.
[38] R.E. Grim, Clay Mineralogy, McGraw Hill, New York, NY, 1968.
[39] L. Michot, F. Villieras, Surface area and porosity, In: F. Bergaya, B.K.G. Theng, G. Lagaly (Eds), Handbook of Clay Science, Elsevier, UK, pp. 965–978, 2006.
[40] E. Bulut, M. Özacar, I.A. Sengil, Equilibrium and kinetic data and process design for adsorption of Congo red onto bentonite, J. Hazard Mater. 154 (2008) 613–622.
[41] M.S. Celik, Electrokinetic behaviour of clay surfaces, In: F. Wypych, K.G. Satyanarayana (Eds), Clay Surfaces Fundamentals and Applications, Interface Science and Technology Series, 1, Elsevier, Amsterdam, pp. 57–89, 2004.
[42] J. Ma, B. Cui, J. Dai, D. Li, Mechanism of adsorption of anionic dye from aqueous solutions onto organobentonite, J. Hazard. Mater. 186 (2011) 1758–1765.
[43] S. Lagergren, Zur theorie der sogenannten adsorption gelöster stoffe. Kungliga Svenska Vetenskapsakademiens [About the theory of so-called adsorption of soluble substances], Handlingar Band 24(4) (1898) 1–39.
[44] Y.S. Ho, G. McKay, Batch lead (II) removal from aqueous solution by peat: Equilibrium and kinetics, Trans I Chem E. 77B (1999) 165–173.

[45] Y.S. Ho, G. McKay, A comparison of chemisorption kinetic models applied to pollutant removal on various sorbents, Trans I Chem E. 76B (1998) 332–339.
[46] N.A. Oladoja, A.K. Akinlabi, Congo red biosorption on palm kernel seed coat, Ind. Eng. Chem. Res. 48 (2009) 6188–6196.
[47] H. Freundlich, Über die Adsorption in Lösungen, Zeitschrift für physikalische Chemie [About the adsorption in solution] 57 (1906) 385–470.
[48] I. Langmuir, The adsorption of gases on plane surfaces of glass, mica, and platinum, J. Am. Chem. Soc. 40 (1918) 1361–1403.
[49] J. Ravichandran, B. Sivasankar, Properties and catalytic activity of acid-modified montmorillonite and vermiculite, Clays Clay Miner. 45 (1997) 854–858.
[50] K.G. Bhattacharyya, S. Sen Gupta, Influence of acid activation of kaolinite and montmorillonite on adsorptive removal of Cd (II) from water, Ind. Eng. Chem. Res. 46 (2007) 3734–3742.
[51] C. Xia, Y. Jing, Y. Jia, D. Yue, J. Ma, X. Yin, Adsorption properties of Congo red from aqueous solution on modified hectorite: Kinetic and thermodynamic studies, Desalination 265 (2011) 81–87.
[52] S. Hong, C. Wen, J. He, F. Gan, Y.S. Ho, Adsorption thermodynamics of methylene blue onto bentonite, J. Hazard. Mater. 167 (2009) 630–633.
[53] M.J. Angove, B.B. Johnson, J.D. Wells, The influence of temperature on the adsorption of cadmium (II) and cobalt (II) on kaolinite, J. Colloid Interface Sci. 204 (1998) 93–103.
[54] F. Tomul, Synthesis, characterization, and adsorption properties of Fe/Cr-pillared bentonites, Ind. Eng. Chem. Res. 50 (2011) 7228–7240.
[55] M. Auta, B.H. Hameed, Modified mesoporous clay adsorbent for adsorption isotherm and kinetics of methylene blue, Chem. Eng. J. 198–199 (2012) 219–227.
[56] Z. Yermiyahu, I. Lapides, S. Yariv, Visible absorption spectroscopy study of the adsorption of Congo red by montmorillonite, Clay Miner. 38 (2003) 483–500.
[57] F. Bergaya, G. Lagaly, M. Vayer, Cation and anion exchange, In: F. Bergaya, B.K.G. Theng, G. Lagaly (Eds), Handbook of Clay Science, Elsevier, UK, 2006, pp. 979–1001.
[58] Y. Fu, T. Viraraghavan, Dye biosorption sites in Aspergillus niger, Bioresour. Technol. 82 (2002) 139–145.